Generalized Rayleigh-Plesset Theory for Cell Size Maintenance in Viruses and Bacteria

Abdul N. Malmi-Kakkada[1], D. Thirumalai[1a]

[1]*Department of Chemistry,*

The University of Texas, Austin, TX 78712

(Dated: February 16, 2019)

[a] Corresponding author: dave.thirumalai@gmail.com

ABSTRACT

The envelopes covering bacterial cytoplasm possess remarkable elastic properties. They are rigid enough to resist large pressures while being flexible enough to adapt to growth under environmental constraints. Similarly, the virus shells play an important role in their functions. However, the effects of mechanical properties of the outer shell in controlling and maintaining the sizes of bacteria or viruses are unknown. Here, we present a hydrodynamic "bubbles with shell" model, motivated by the study of bubble stability in fluids, to demonstrate that shell rigidity and turgor pressure control the sizes of bacteria and viruses. A dimensionless compliance parameter, expressed in terms of the Young's modulus of the shell, its thickness and the turgor pressure, determines membrane response to deformation and the size of the organisms. By analyzing the experiment data, we show that bacterial and viral sizes correlate with shell elasticity, which plays a critical role in regulating size.

Viruses consist of genetic material surrounded by a protective coat of proteins called capsids, which withstand high osmotic pressures and undergo modification (or maturation) to strengthen capsids after viral assembly (1). The protective coat is critical in enabling the virus to maintain its functionally intact state. In bacteria, the envelope covering the cytoplasm, besides being essential in sustaining the shape of the cell, protects the bacteria from adversary factors such as osmotic shock and mechanical stress (2–4). Bacterial cell wall is composed mostly of peptidoglycan, whose synthesis, regulation and remodeling are central to bacterial physiology (5). Growing body of evidence suggests that proteins controlling the organization of peptidoglycan growth could be crucial in the maintenance of cell size (2, 6). Bacteria and viruses exhibit remarkable diversity in size and shape. Nevertheless, for the purposes of developing a physical model, we picture them as envelopes enclosing the material necessary for sustaining their lives.

Individual strains of bacteria are known to maintain a narrow distribution of size even when they divide multiple times (7–9). A number of physical models exploring how microorganisms maintain size and shape have been proposed (10–13), with similarities between cell elongation and bubble dynamics (10, 11). Historically, cell size maintenance has been discussed in terms of two major models: "timer," where cells grow for a fixed amount of time before division, and "sizer," where cells commit to division at a critical size (14). Another important model is the "adder" mechanism, which proposes that a constant size is added between birth and division (8, 15, 16). These models incorporate a 'license to divide' approach (17) - depending upon whether passage of time, growth to a specific size or addition of fixed size are necessary in order to trigger cell division and regulate size. Recently, the need to attain a steady state surface area to volume ratio was highlighted as the driving factor behind size homeostasis in bacteria (18). In emphasizing the need to move away from a 'birth-centric' picture, alternate models relating volume growth to DNA replication initiation have been proposed (9, 19) based on experiments (20, 21). Despite significant advances in understanding size homeostasis, the influence of important physical parameters of the cell such as the turgor pressure and elastic properties of their outer envelope on size maintenance is unknown. Even though the molecules

that control cell cycle and division have been identified (22), the ability to predict size from first principles remains a challenging problem.

Here, we develop an entirely different approach by turning the mechanism of size maintenance into an instability problem in hydrodynamics. We begin by studying the deformation response modes of the cell wall using a generalization of the Rayleigh-Plesset (RP) equation, which was derived in the context of modeling the dynamics of bubbles in fluids (23). The RP equation is a special case of the Navier-Stokes equation used to describe the size of a spherical bubble whose radius is R. We use the term "shell" generically, being equally applicable to membrane, the composite layers making up the bacterial envelope or capsids. In our theory, the shell subject to deformation (e.g. expansion) exhibits two fundamental response modes: (i) elastic mode, where perturbative deformation of the cell wall is followed by initial size recovery, and (ii) unstable response where minute deformation results in continuous growth of the deformation. The initial size is not recovered in the unstable response mode, hence we refer to it as the plastic response. This is similar to the yield point in springs beyond which original length of the spring is not recovered after stretching. The importance of these two fundamental deformation response modes in the context of bending and growth in rod shaped cells was investigated recently (24).

A key prediction of our theory is the relation between the deformation response modes and optimal size, dictated by a single dimensionless compliance parameter, ζ, expressed in terms of the elasticity of the shell and the turgor pressure. We show that an optimal cell size requires that ζ strike a balance between elastic and plastic response to deformation, thus maintaining microorganisms at the edge of stability. The model consistently predicts the size of sphere-like bacteria and viruses given the physical properties of the cell and the protecting shell.

Approximating bacteria and viruses as bubbles with shells enables us to approach the problem of size maintenance using a generalized Rayleigh-Plesset (RP) equation (see Fig. 1). For a spherical bubble of radius, $R(t)$, in a liquid at time t, the temperature and pressure outside the bubble, T_{out} and p_{out}, are assumed to be constant. The liquid mass density, ρ and the kinematic viscosity, ν, are also taken to be constant and uniform. If we assume that the contents of

the bubble are at a constant temperature and exert steady osmotic pressure on the bubble wall, p_{in}, then the effect of the turgor pressure may be taken into account. We outline in the Supplementary Information (SI) that the RP equation is motivated from the general equations governing fluid flow - the continuity and the Navier-Stokes equations. To extend the RP equation to study the size maintenance mechanism in microorganisms, an additional term for the bending pressure of the thin outer shell is required. The elastic energy (per unit area) of bending a thin shell is proportional to the square of the curvature (25). Thus, the generalized RP equation is,

$$\frac{p_{in}(t) - p_{out}(t)}{\rho} + \frac{Yh^2}{\rho R^2} = R\frac{d^2R}{dt^2} + \frac{3}{2}(\frac{dR}{dt})^2 + \frac{4\nu}{R}\frac{dR}{dt} + \frac{2S}{\rho R}, \tag{1}$$

where Yh^2/R^2 is the bending pressure of the elastic shell, Y is the Young's modulus, h is the thickness of the shell, and S is the surface tension acting on the shell. The bending pressure, or the resistance to bending, arises due to the outer side of a bent material being stretched while the inner side is compressed (see Inset in Fig. 1). For more details on the bending pressure term see SI Section I. The first term on the left hand side accounts for the pressure difference between inside and outside of the cell and the other terms involve time derivatives of the radius.

Shell displacement, $\delta R(t)$, in the radial direction leads to $R(t) = R_e + \delta R(t)$, where R_e is a constant. If $\delta R/R_e << 1$, an equation for $\delta R(t)/R_e$ may be derived,

$$\frac{d^2\delta\bar{R}}{d\bar{t}^2} + 4\frac{d\delta\bar{R}}{d\bar{t}} = 2\delta\bar{R}(\bar{S} - \bar{Y}\bar{h}^2), \tag{2}$$

in non-dimensional units where $\delta\bar{R} = \delta R/R_e$, $\bar{h} = h/R_e$. We choose $\tau = R_e^2/\nu$ which sets the time unit and R_e (the mean cell size) is the unit of length. Similarly, the Young's modulus ($\bar{Y}$) and surface tension are rescaled using $p_r = \frac{\rho R_e^2}{\tau^2}$ and $\bar{S} = S/(p_r R_e)$. Three types of temporal behavior in $\delta\bar{R}$ are illustrated in Fig. 2, where the radial displacement either increases, stays constant or decays. Both analytic and numerical solutions, with initial conditions $\delta\bar{R}(\bar{t} = 0) = 0.01$, $d\delta\bar{R}/d\bar{t}(\bar{t} = 0) = 0$, may be readily obtained, as detailed in the SI. Fig. 2a shows that as the dimensionless surface tension ($\bar{S}$) increases, the behavior of $\delta R(t)/R_e$ changes from continuous decay to growth. In Fig. 2b, $\bar{S}$ is kept constant while the stiffness of the shell is varied. Time dependent perturbative displacement, $\delta R(t)/R_e$, once again shows three distinct trends as the

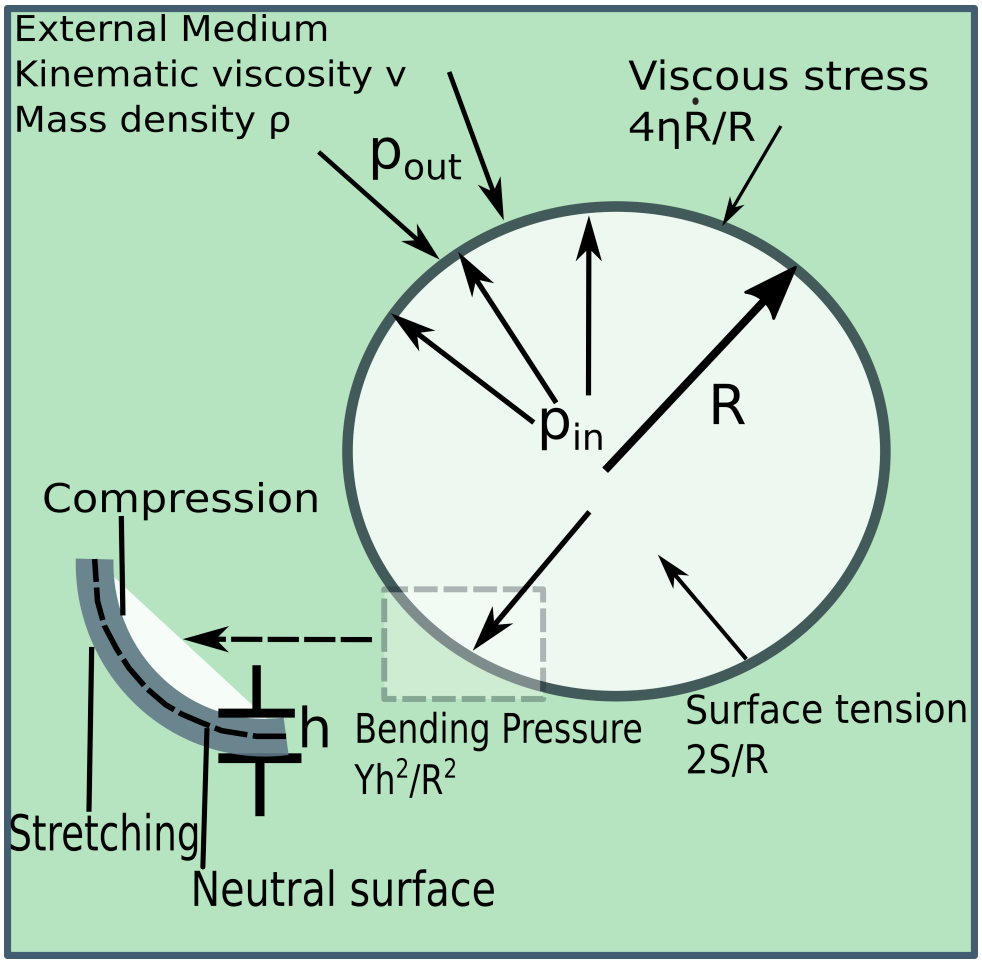

FIG. 1: Illustration of the model cell based on the RP equation. The cell wall is a thin shell of thickness h. The stresses acting on the cell wall are labeled. Viscosity of the surrounding medium is $\eta = \nu\rho$.

shell stiffness, $\bar{Y}$, increases. Since $\delta R/R_e$ is the strain experienced by the elastic shell due to infinitesimal deformation, these response modes signify a transition between the 'elastic' and the 'plastic' regime. The plastic regime corresponds to incremental growth in strain while in the elastic regime the strain decays to zero over time, implying that the cell size is maintained.

The strain response modes depend on whether S is greater than or less than Yh^2/R_e (see Eq. 2). If $S > Yh^2/R_e$, continuous growth in strain results in the 'plastic' regime. However, if $S < Yh^2/R_e$, a decaying solution for the strain leads to the 'elastic' regime. The critical value of the surface tension that dictates the boundary between the two regimes is predicted to be at

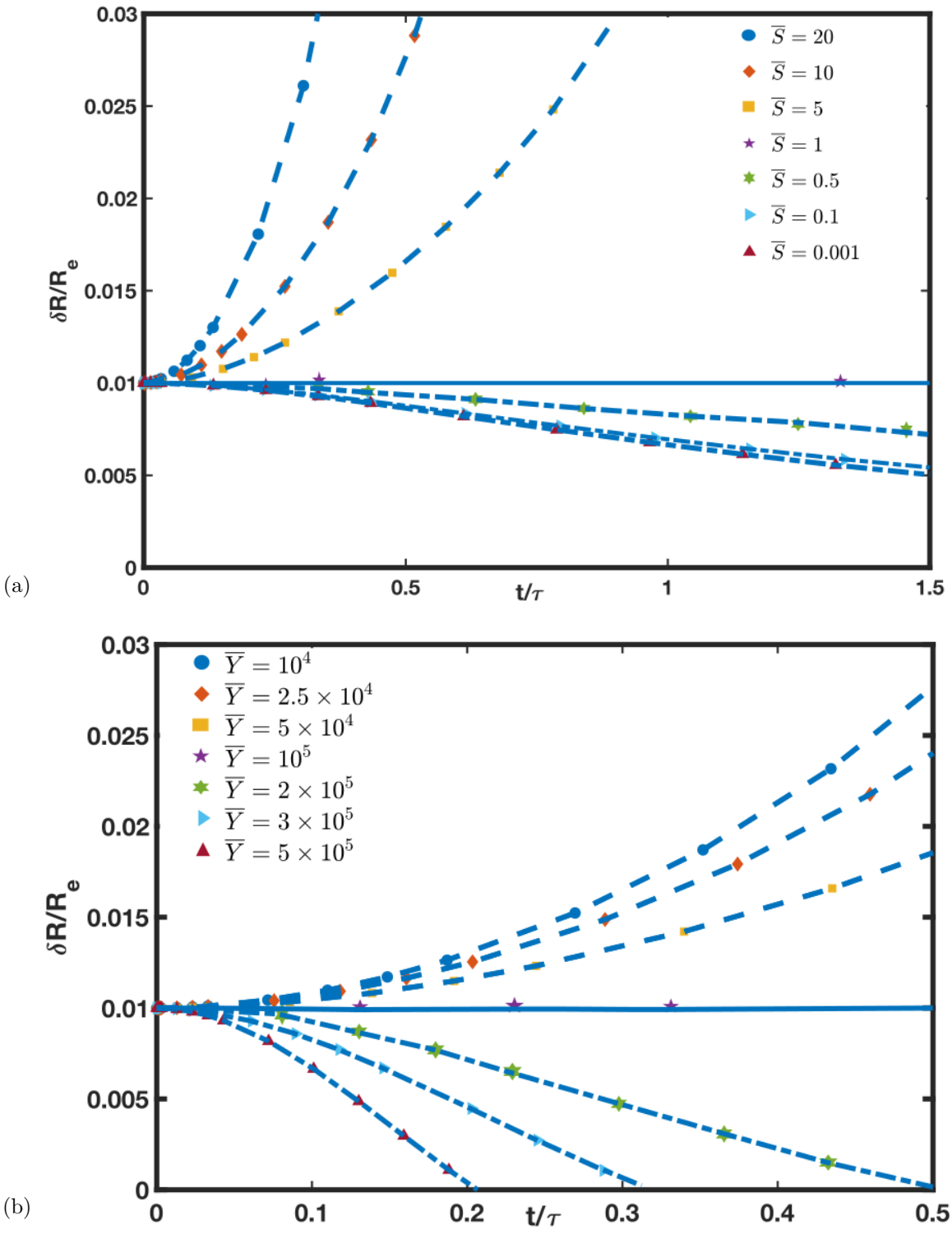

FIG. 2: Solutions (a) for the first order RP equation shows the time dependent behavior of strain. Time is scaled by τ and length by R_e. $\bar{Y} = 10^4$ and $\bar{h} = 10^{-2}$ are kept constant while $\bar{S}$ is varied. (b) Same as in (a) with $\bar{S} = 10$ and $\bar{h} = 10^{-2}$ kept constant while $\bar{Y}$ is varied.

$\bar{S}_c = \bar{Y}\bar{h}^2$. In Fig. 2a, for $\bar{Y} = 10^4$ and $\bar{h} = 10^{-2}$, the critical surface tension corresponds to $\bar{S}_c = 1$. Similarly in Fig. 2b, we show that the critical elastic modulus is $\bar{Y}_c = \bar{S}/\bar{h}^2 = 10^5$, in agreement with numerical results. Note that Table I in the SI shows that the parameter ranges considered are physiologically relevant. Surface tension forces must be explicitly taken into account in studying envelope deformation of bacteria and viruses. The mechanical equilibrium of bacterial shells is determined by surface tension (26, 27). Similarly, mechanical properties of viral capsids are determined by surface tension (28) or effective surface tension-like terms (1).

An important prediction of the theory is that the dimensionless compliance parameter, ζ, quantifies the shell response to perturbative deformation and thereby sets a universal length scale for the size of microorganisms. The parameter ζ depends on intrinsic physical properties of the cell, which collectively play an important role in the how bacterial cell wall deforms as well as the pressure differential across the shell. The details of the derivation of,

$$\zeta = \frac{Yh^2}{\Delta P R^2}, \tag{3}$$

where $\Delta P = p_{in} - p_{out}$, are given in the SI. The compliance parameter in Eq. 3 may be obtained by equating the bending pressure ($\sim Yh^2/R^2$ - this form is justified in the SI) and the contribution arising from surface tension ($\sim S/R$, the last term in Eq. 1). By using the Young-Laplace equation for $S \sim \Delta P R$, we obtain Eq. 3.

Interestingly, the same parameter rewritten as, $\kappa = 1/\zeta$, was found to be important in distinguishing between bending and tension-dominated response of the bacterial wall during the indentation of *Magnetospirillum gryphiswaldense* with an AFM tip (27). In a more recent study (24), the dimensionless variable χ (related to the compliance parameter by $\chi(R/h) = 1/\zeta$), was shown to demarcate the boundary between elastic and plastic deformation regimes for cylindrical bacteria.

The elastic regime corresponds to $\zeta > 1$, while for $\zeta < 1$ the deformation is plastic. Since plastic and elastic deformation modes are expected to be of comparable importance in bacterial cell walls (24), we anticipate that the condition $\zeta = 1$ could play an important role in determining size. Note that $\zeta = 1$ corresponds to $\delta R(t)/R_e =$ constant with neither decay nor growth in

response to perturbative displacement. Thus, the boundary between the plastic and elastic regime ($\zeta = 1$) lets us identify a critical radius,

$$R_c^2 \sim \frac{Yh^2}{\Delta P}, \tag{4}$$

which is the central result of our work. The consequences of Eq. 4 are explored by analyzing experimental data.

The critical radius obtained above unveils the universal dependence of the size of microorganisms on the intrinsic physical parameters of the cell and its outer shell - the pressure difference between inside and outside, and the Young's modulus and the thickness of the shell, respectively. We now analyze the size of bacteria (*S. aureus, E. coli, B. subtilis*), and viruses (*Murine Leukemia Virus (MLV)* and Φ*29 bacteriophage*) in relation to their shell physical properties. Data for the radius, elastic modulus, shell thickness and pressure difference were obtained from the literature. A comparison of the shell thickness, h, to the radial size, R, for 12 bacteria and viruses is presented in Fig. 3a. The thickness of the cell wall (Eq. 3) given by,

$$h \sim \sqrt{\zeta(\frac{\Delta P}{Y})}R, \tag{5}$$

directly proportional to size. Remarkably, the ratio of the turgor pressure to shell stiffness, $\Delta P/Y \sim 10^{-2}$ (see Inset Fig. 3a), falls on a straight line. In agreement with our theory, the shell thickness is linearly correlated to the overall size with the Pearson correlation coefficient, $r = 0.73$. As predicted by the theory, the data points lie close to $\zeta = 1$ (marked by the dashed line) in Fig. 3a, indicative of the importance of the balance between plastic and elastic deformation modes in microorganisms. Similarly, the relation between turgor pressure and shell Young's modulus can be predicted using,

$$Y \sim \zeta(\frac{R}{h})^2\Delta P. \tag{6}$$

Taking the ratio between radial size and shell thickness, $(R/h)^2 \sim 10^2$ (see Inset Fig. 3b), allows us to identify the preferable ζ regime. The Pearson correlation coefficient, $r = 0.74$, and the region where $\zeta = 1$ is marked by a dashed line in Fig. 3b. When either ΔP or Y were not available, value of a similar species was used (see Table II in SI for more details).

Bacteria: We propose that the physical mechanism of adapting to a specific value of ζ could be utilized by bacteria and viral particles to tightly maintain a specific size. We examine the consistency of this proposal by analyzing experimental data. The thickness of the *S. aureus* cell wall is tuned to higher values as a result of nutrient depletion in the stationary phase (in *S. aureus* synthetic medium) (29). Glycine depletion in the nutrient medium forces *S. aureus* to make "imperfect" peptidoglycan resulting in a less rigid cell wall, which is more susceptible to lysis (30). *S. aureus* responds by increasing the peptidoglycan thickness. The observed adaptation behavior of the cell wall thickness is to be expected from Eq. (4). Given a decrease in Y (due to a defective cell wall) and assuming that the ratio of pressure difference to Y is a constant, the bacteria can maintain its size by increasing the thickness, h. A scaling behavior obtained earlier by balancing the bending pressure of shells with turgor pressure (12) showed that R/h is proportional to $(Y/\Delta P)^{1/3}$, focusing on alga cells and fungi. This proposed scaling arises due to surface tension-like forces not being considered, which perhaps accounts for the departure from the proposed scaling for bacteria and viruses (the focus of this study). We quantitatively compare the best fit to experimental data presented in Fig. 3a to the two different scaling behaviors: (i) $h = \sqrt{\zeta(\Delta P/Y)}\ R$, and (ii) $h = \alpha^{-1}(\Delta P/Y)^{1/3}\ R$ (12) and show that the experimental data is better accounted by the generalized RP theory (see SI section VI).

Maturation of Viruses: We now explore the role of ζ (Eq. 3) in the viral maturation process. Double stranded (ds) DNA bacteriophages are known to undergo conformational and chemical changes that tend to strengthen the shell (1) by a process that resembles structural phase transition in crystals. This is necessary considering that the shells have to be able to withstand large internal pressures and at the same time be unstable so that their genome can be released into host cells during infection. The radius of a viral particle remains approximately constant throughout its life cycle. However, experimental evidence shows that shell thickness of viruses is tuned actively (see Table II in SI and references therein). In *HIV, MLV* and *HK97* viruses, the shell thickness decreases during the maturation process (31–33). Interestingly, in *MLV* and *HK97* the decrease in shell thickness corresponds to an increase in capsid stiffness (32, 33).

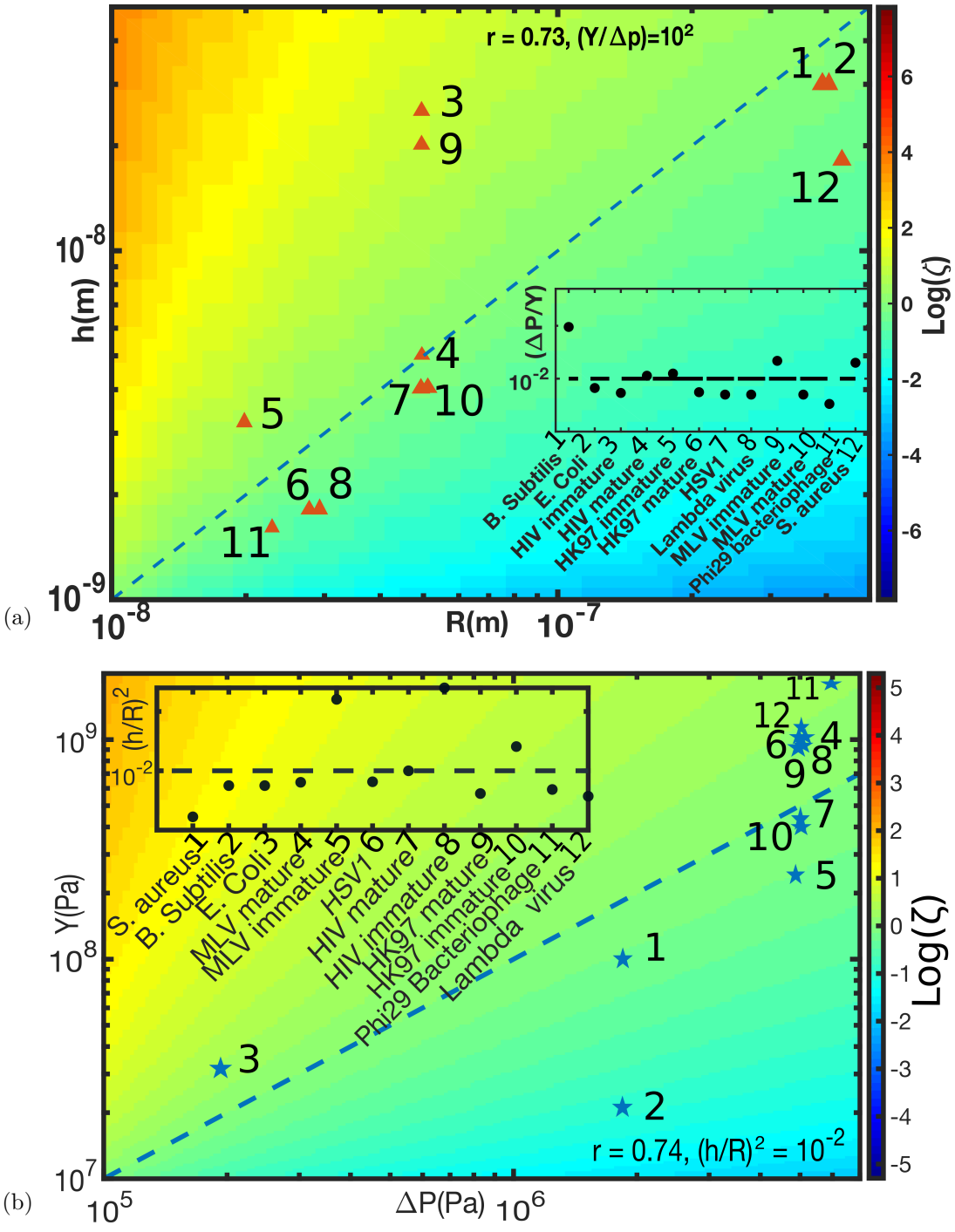

FIG. 3: (a) Test of the relation given in Eq. (5) for different bacteria and viruses. Inset shows the ratio $\Delta P/Y$. (b) Trend in shell Young's modulus (Y) versus turgor pressure (ΔP) in units of Pa. Inset shows the ratio of $(h/R)^2$. The data were compiled from existing literature. Calculated ζ (in log scale, with fixed $\Delta P/Y = 10^{-2}$ in (a) and $(R/h)^2 = 10^2$ in (b)) is indicated in color heat map on the right of the figures. The dashed line in the figure marks $\zeta = 1$.

Given these clues, we quantify the role of ζ in the viral maturation process. Fig. 4 compares the size and shell elastic properties of individual viruses between their immature and mature phases. The tuning of the ratio of radius to the shell thickness as the virus matures can be clearly observed (filled $\rightarrow$ hollow shapes). As the viral particle matures, a transition from the elastic regime($\zeta > 1$) to a plastic regime($\zeta \leq 1$) is observed. The inset in Fig. 4 shows the fractional change in the compliance, $\delta\zeta/\zeta = (\zeta_{immature} - \zeta_{mature})/\zeta_{immature}$. Notable change in ζ due to maturation occurs for all three viruses with $\zeta_{mature} << \zeta_{immature}$. This marks a crossover behavior in the viral lifecycle where surface tension-like forces in the shell begin to dominate the force associated with the shell stiffness. As before, the dashed line in the figure ($\zeta = 1$) separates the elastic regime from the plastic regime.

The elastic modulus (Y) of the viral shell is an important parameter in the maturation process of viruses. Shells of *MLV* and *HK97* become stiffer as they mature. As a result of the increased shell stiffness, h decreases while maintaining approximately the same size. In the three different viruses analyzed, ζ approaches 1, which we propose to be a general property of viral maturation.

By generalizing a hydrodynamic model based on the Rayeigh-Plesset equation, originally formulated in the context of bubbles in fluids, we proposed a novel unified framework to predict the size of bacteria and viruses from first principles. Given the shell elastic properties and the pressure differential between the inside and outside, the importance of selecting a deformation response mode is shown as a possible mechanism to constrain size. Nanoscale vibrations, proposed as a signature of life (35), could provide a natural basis for bacteria and viruses to detect the elasticity of shells. We identified a compliance parameter, ζ, in terms of the physical properties of the cell as the most relevant variable controlling cell size. Viral particles are especially sensitive to ζ, and we predict that shell properties evolve to minimize ζ during maturation. By merging approaches from hydrodynamics and elasticity theory, we have proposed a new mechanism for an important question in cell biology pertaining to size regulation. In conjunction with studies on the role of biochemical processes in shape and size maintenance, the importance of physical parameters should also be considered in order to fully understand size homeostasis in

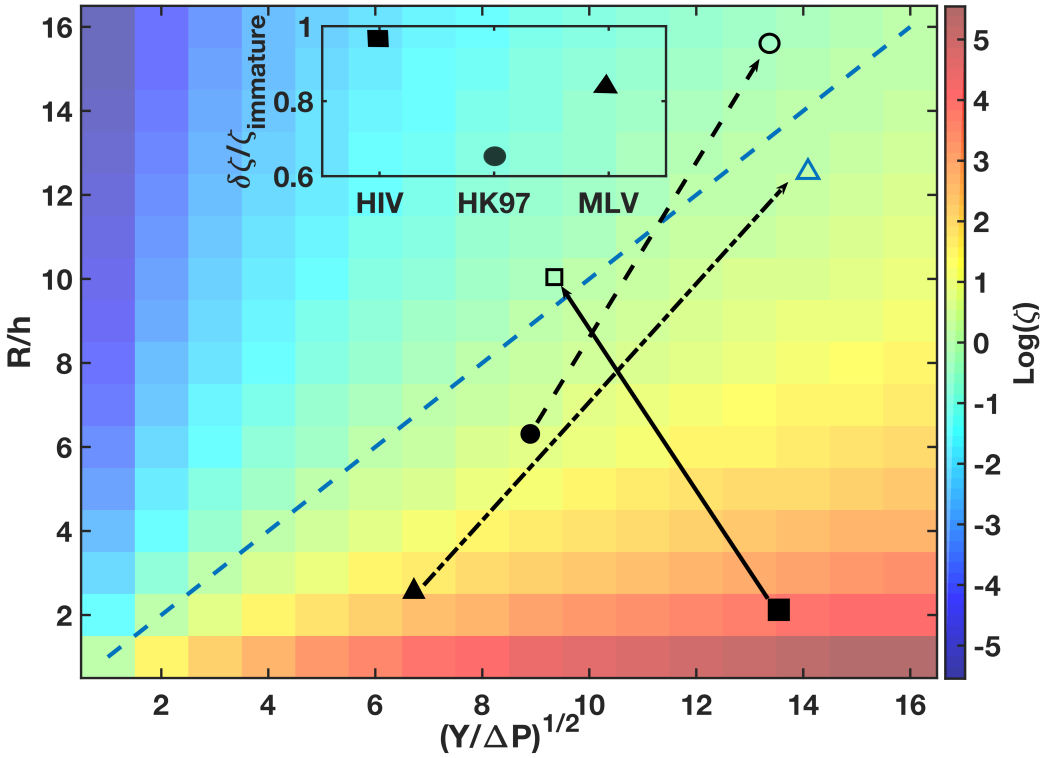

FIG. 4: Comparing the ratio of R/h to $(Y/\Delta P)^{1/2}$ during the immature and mature stages of viruses. Mature/Immature HIV (□) (31), Mature/Immature HK97 virus (◯) (33, 34), Mature/Immature Murine Leukemia Virus (MLV △) (32). Hollow and filled symbols correspond to mature and immature viruses respectively (with lines joining them as guides to the eye). Calculated ζ is indicated in color scale on the right. The dashed diagonal line in the figure marks $\zeta = 1$. Lines connecting filled to hollow symbols visualize the tuning of the physical parameters as a virus matures.

bacteria and viruses.

Acknowledgements: This work was supported by the National Science Foundation through NSF Grant No. PHY 17-08128. Additional support was provided by the Welch Foundation through the Collie-Welch Chair (F-0019). We are grateful to Mauro Mugnai, and Xin Li for discussions and comments on the manuscript.

Data availability: The authors declare that the data supporting the findings of this study are available within the paper [and its supplementary information files].

Competing financial interests: The authors declare no competing financial interests.

[1] WH Roos, R Bruinsma, and GJL Wuite. Physical virology. *Nature physics*, 6(10):733, 2010.

[2] Hannah H Tuson, George K Auer, Lars D Renner, Mariko Hasebe, Carolina Tropini, Max Salick, Wendy C Crone, Ajay Gopinathan, Kerwyn Casey Huang, and Douglas B Weibel. Measuring the stiffness of bacterial cells from growth rates in hydrogels of tunable elasticity. *Molecular microbiology*, 84(5):874–891, 2012.

[3] Enrique R Rojas, Kerwyn Casey Huang, and Julie A Theriot. Homeostatic cell growth is accomplished mechanically through membrane tension inhibition of cell-wall synthesis. *Cell systems*, 5(6):578–590, 2017.

[4] Lisa Willis and Kerwyn Casey Huang. Sizing up the bacterial cell cycle. *Nat. Rev. Microbiol.*, 15(10):606–620, 2017.

[5] Waldemar Vollmer, Didier Blanot, and Miguel A De Pedro. Peptidoglycan structure and architecture. *FEMS microbiology reviews*, 32(2):149–167, 2008.

[6] Nikolay Ouzounov, Jeffrey P Nguyen, Benjamin P Bratton, David Jacobowitz, Zemer Gitai, and Joshua W Shaevitz. Mreb orientation correlates with cell diameter in escherichia coli. *Biophysical journal*, 111(5):1035–1043, 2016.

[7] Stephen Cooper. *Bacterial growth and division: biochemistry and regulation of prokaryotic and eukaryotic division cycles*. Elsevier, 2012.

[8] Ariel Amir. Cell size regulation in bacteria. *Physical Review Letters*, 112(20):208102, 2014.

[9] Po-Yi Ho and Ariel Amir. Simultaneous regulation of cell size and chromosome replication in bacteria. *Frontiers in microbiology*, 6:662, 2015.

[10] DW Thompson. On growth and form, abridged ed. *Cambridge: Cambridge University.(Original work published 1917)*, 1961.

[11] AL Koch, ML Higgins, and RJ Doyle. Surface tension-like forces determine bacterial shapes: Streptococcus faecium. *Microbiology*, 123(1):151–161, 1981.

[12] Arezki Boudaoud. Growth of walled cells: from shells to vesicles. *Physical review letters*, 91(1):018104, 2003.

[13] Shiladitya Banerjee, Norbert F Scherer, and Aaron R Dinner. Shape dynamics of growing cell walls. *Soft matter*, 12(14):3442–3450, 2016.

[14] Suckjoon Jun and Sattar Taheri-Araghi. Cell-size maintenance: universal strategy revealed. *Trends in microbiology*, 23(1):4–6, 2015.

[15] L Sompayrac and O Maaløe. Autorepressor model for control of dna replication. *Nature New Biology*, 241(109):133, 1973.

[16] Sattar Taheri-Araghi, Serena Bradde, John T Sauls, Norbert S Hill, Petra Anne Levin, Johan Paulsson, Massimo Vergassola, and Suckjoon Jun. Cell-size control and homeostasis in bacteria. *Current Biology*, 25(3):385–391, 2015.

[17] Manuel Campos, Ivan V Surovtsev, Setsu Kato, Ahmad Paintdakhi, Bruno Beltran, Sarah E Ebmeier, and Christine Jacobs-Wagner. A constant size extension drives bacterial cell size homeostasis. *Cell*, 159(6):1433–1446, 2014.

[18] Leigh K Harris and Julie A Theriot. Relative rates of surface and volume synthesis set bacterial cell size. *Cell*, 165(6):1479–1492, 2016.

[19] Ariel Amir. Point of view: Is cell size a spandrel? *Elife*, 6:e22186, 2017.

[20] Stephen Cooper and Charles E Helmstetter. Chromosome replication and the division cycle of escherichia coli br. *Journal of molecular biology*, 31(3):519–540, 1968.

[21] Mats Wallden, David Fange, Ebba Gregorsson Lundius, Özden Baltekin, and Johan Elf. The synchronization of replication and division cycles in individual e. coli cells. *Cell*, 166(3):729–739, 2016.

[22] Wallace F Marshall, Kevin D Young, Matthew Swaffer, Elizabeth Wood, Paul Nurse, Akatsuki Kimura, Joseph Frankel, John Wallingford, Virginia Walbot, Xian Qu, et al. What determines cell size? *BMC biology*, 10(1):101, 2012.

[23] Christopher Earls Brennen and Christopher E Brennen. *Fundamentals of multiphase flow*. Cambridge university press, 2005.

[24] Ariel Amir, Farinaz Babaeipour, Dustin B McIntosh, David R Nelson, and Suckjoon Jun. Bending forces plastically deform growing bacterial cell walls. *Proceedings of the National Academy of Sciences*, page 201317497, 2014.

[25] Markus Deserno. Fluid lipid membranes–a primer. *See http://www. cmu. edu/biolphys/deserno/pdf/membrane_theory. pdf*, 2007.

[26] Yi Deng, Mingzhai Sun, and Joshua W Shaevitz. Direct measurement of cell wall stress stiffening and turgor pressure in live bacterial cells. *Physical Review Letters*, 107(15):158101, 2011.

[27] Markus Arnoldi, Monika Fritz, Edmund Bäuerlein, Manfred Radmacher, Erich Sackmann, and Alexei Boulbitch. Bacterial turgor pressure can be measured by atomic force microscopy. *Physical Review E*, 62(1):1034, 2000.

[28] Roya Zandi and David Reguera. Mechanical properties of viral capsids. *Physical Review E*, 72(2):021917, 2005.

[29] Xiaoxue Zhou and Lynette Cegelski. Nutrient-dependent structural changes in s. aureus peptidoglycan revealed by solid-state nmr spectroscopy. *Biochemistry*, 51(41):8143–8153, 2012.

[30] Bruce Hofkin. *Living in a microbial world*. Garland Science, 2010.

[31] Nitzan Kol, Yu Shi, Marianna Tsvitov, David Barlam, Roni Z Shneck, Michael S Kay, and Itay Rousso. A stiffness switch in human immunodeficiency virus. *Biophysical journal*, 92(5):1777–1783, 2007.

[32] Nitzan Kol, Micha Gladnikoff, David Barlam, Roni Z Shneck, Alan Rein, and Itay Rousso. Mechanical properties of murine leukemia virus particles: effect of maturation. *Biophysical journal*, 91(2):767–774, 2006.

[33] Wouter H Roos, Ilya Gertsman, Eric R May, Charles L Brooks, John E Johnson, and Gijs JL Wuite. Mechanics of bacteriophage maturation. *Proceedings of the National Academy of Sciences*, 109(7):2342–2347, 2012.

[34] John E Johnson. Virus particle maturation: insights into elegantly programmed nanomachines. *Current opinion in structural biology*, 20(2):210–216, 2010.

[35] Sandor Kasas, Francesco Simone Ruggeri, Carine Benadiba, Caroline Maillard, Petar Stupar, Hlne Tournu, Giovanni Dietler, and Giovanni Longo. Detecting nanoscale vibrations as signature of life. *Proceedings of the National Academy of Sciences*, 112(2):378381, 2014.